ORIGINAL CONTRIBUTION

Nonlinear viscoelastic characteristic investigations of waxy crude oils under stress-controlled large amplitude oscillatory shear (LAOStress)

Hongfei Liu[1,2] · Hongying Li[1] · Yang Zhao[3] · Xuefeng Wang[4] · Huiyuan Li[1,5] · Jinjun Zhang[1]

Abstract

Gelled waxy crude oils can be considered as an elasto-viscoplastic material, exhibiting the transition from linear to nonlinear viscoelasticity. The LAOStress measurements have rarely been applied in the crude oil rheology literature to investigate the nonlinear viscoelasticity. In this study, we present results of the nonlinear viscoelastic characteristics under LAOStress by a series of analytical methods of Fourier transform rheology, Chebyshev strain decomposition, Lissajous curves analysis, energy dissipation calculation, viscoelastic measures quantification, and Pipkin diagram interpretation. Both the elastic and viscous nonlinearities were found to be first strengthened before yielding and subsequently weakened after yielding with the increase in imposed stress amplitude σ_0, and a more striking nonlinear response can be captured when using a lower angular frequency ω. However, the defined viscoelastic measures and energy dissipation characteristics continue to keep getting more significant with increasing σ_0, even after structural fracture. The results of Lissajous curves analysis reflect that a lower applied ω is more favorable for the structural nonlinear destruction and thus flowability enhancement of interlocking waxy network. The Pipkin diagrams were finally plotted to represent the nonlinear rheological signatures to an oscillatory input, showing a higher measured yield stress under a higher imposed ω.

Keywords Waxy crude oil · LAOStress · Nonlinear viscoelasticity · Fourier transform rheology · Lissajous curve

Introduction

Waxy crude oils represent a significant amount of the petroleum reserves and productions in the world, and the transportation of waxy crude oils through pipelines is an industrial practice that requires great attention (Vinay et al. 2007; Mendes et al. 2017). As noted by many research results (Chang et al. 1998; Dimitriou and Mckinley 2014; Mendes et al. 2015), wax can exist in different forms, which makes waxy crude oils exhibit very complicated temperature-dependent rheological properties. When the temperature is higher than the wax appearance temperature (WAT), wax is dissolved in liquid oil and the waxy crude oil behaves as Newtonian fluid. As the temperature drops below the WAT, wax crystals will precipitate out and be suspended in liquid oil, causing the crude oil gradually change into non-Newtonian fluid. Upon further cooling, the precipitated wax crystals will interlock and develop spongy-like crystal networks, and the liquid oil will be entrapped into the wax crystal structure, resulting in the formation of waxy gels. The gelled waxy crude oil can be considered as an elasto-viscoplastic material, featuring complex non-Newtonian rheological characteristics, such as viscoelasticity and yield stress (Chang et al. 1999; Kané et al. 2004).

The widely accepted mechanism for the viscoelasticity of gelled waxy crude oils can be explained as follows. The precipitated wax crystals attract with each other by van der

✉ Hongying Li
lihy314@163.com

✉ Jinjun Zhang
zhangjj@cup.edu.cn

1 National Engineering Laboratory for Pipeline Safety/MOE Key Laboratory of Petroleum Engineering/Beijing Key Laboratory of Urban Oil & Gas Distribution Technology, China University of Petroleum Beijing, Beijing 102249, China

2 China National Aviation Fuel International Holdings Limited, Beijing 100029, China

3 PipeChina Oil & Gas Control Center, Beijing 100007, China

4 PetroChina Jidong Oilfield Company, Tangshan 063299, China

5 CNPC Research Institute of Safety & Environment Technology, Beijing 102206, China

Waals force and then interact with each other in the space, and the aggregation of wax crystals is responsible for the three-dimensional network structure formation (Wardhaugh and Boger 1991; Visintin et al. 2005). On the one hand, the network structure has the ability to prevent the flow of liquid oil. On the other hand, the elastic deformation of the network structure can be generated under the action of external force. Therefore, the whole waxy gel systems exhibit the viscoelastic behavior (da Silva and Coutinho 2004).

Understanding the viscoelasticity of gelled waxy crude oils is of significance for developing robust elasto-viscoplastic constitutive model, and the establishment of the constitutive model for waxy crude oils is both the goal for the investigation of crude oil rheology and the indispensable procedure for the hydraulic computation of pipeline start-up flow which is one of the most concern problems of flow assurance. However, so far the viscoelasticity of waxy crude oils has not been thoroughly studied. As a result, most researchers (Barnes 1997; Mujumdar et al. 2002; Teng and Zhang 2013) often simplify the waxy crude oil as a viscoplastic material and use the yield stress to characterize the starting point of structural damage. Roughly, only at stress above the yield stress, will the flow of waxy crude oils occur because of structural fracture. When the applied stress is lower than the yield stress, it is assumed that no structural deformation happens, which is clearly inconsistent with the actual loading process. From the above analysis, it can be seen that the development of the investigation for the viscoelasticity of waxy crude oils is extremely necessary both for the scientific research and engineering practice.

Dynamic oscillatory shear experiment as an effective technique is usually employed to study the viscoelasticity of structured materials (Wardhaugh and Boger 1991; Chang et al. 1998; Visintin et al. 2005; Abivin et al. 2012). By dynamic oscillatory shear experiments, both the elastic and viscous properties can be studied over a wide range of oscillatory amplitudes and frequencies. According to the amplitude of the imposed oscillatory stress/strain, dynamic oscillatory shear experiment can be divided into small amplitude oscillatory shear (SAOS) and large amplitude oscillatory shear (LAOS) (Hyun et al. 2011). The SAOS experiment is the rheological experimental method to study the linear viscoelasticity of waxy crude oils, whereas LAOS is always used to study the nonlinear viscoelastic properties.

In the studies of the dynamic viscoelasticity, most attention has been paid to the linear viscoelastic region. The linear viscoelastic properties of waxy crude oils have been widely investigated by SAOS, such as using temperature sweep to determine the gelation temperature (Kané et al. 2004; Visintin et al. 2005), using time sweep to monitor the aging process during isothermal holding (da Silva and Coutinho 2004) and structural recovery behaviors after the cessation of shear (Visintin et al. 2005; Lionetto et al. 2007),

using frequency sweep to obtain the linear viscoelastic spectra of waxy crude oils (Kané et al. 2004; Ilyin and Strelets 2018). Wardhaugh and Boger (1991) demonstrated that when the waxy crude oil behaves within the linear viscoelastic region, the dependencies of strain on stress amplitude show a good linear relation. In addition, Chang et al. (1998) pointed out that the linear response could only occur with an oscillatory stress amplitude lower than the elastic limit yield stress, which is one of the three yield stresses proposed by Chang et al. to divide the yielding process of waxy crude oils.

The boundary of the linear viscoelastic region and nonlinear region can be characterized by the parameters of critical linear stress and critical linear strain. According to our previous work, both the critical linear stress and critical linear strain are found to be independent of the rheological experimental methods (Rønningsen 1992; Tarcha et al. 2015; Liu et al. 2018). Using stress ramp (Hou 2012) and dynamic stress sweep experiments (Webber 2000; Li et al. 2009), some research reported that the critical linear stress increases with the decrease in temperature, while the critical linear strain decreases.

While the imposed stress (strain) amplitude is above the critical linear stress (strain), the rheological responses of the gelled waxy crude oils start to evolve toward the nonlinear viscoelastic region. Many researchers (Wardhaugh and Boger 1991; Tiu et al. 2006; Ewoldt et al. 2008) reported that the curves of stress–strain in the nonlinear region deviate from the linear relationship, and meanwhile, G' and G'' start to decrease gradually. Compared to the application of SAOS in the study of waxy crude oil viscoelasticity, LAOS is less used in the crude oil rheology, except for the limited number of work. Dimitriou and Mckinley (2014) conducted strain-controlled large amplitude oscillatory shear (LAOStrain) measurements to study the nonlinear viscoelasticity of model crude oil by imposing an oscillatory deformation with the form of $\gamma(t) = \gamma_0 sin\omega t$ and further analyzed the Lissajous curves (the measured stress σ plotted against the sinusoidally varying strain $\gamma(t)$). Their study showed that at low values of γ_0, the response of the oil sample is that of a linear viscoelastic solid, and the Lissajous curve exhibits an elliptical shape. As γ_0 is progressively increased, the characteristic shape of the Lissajous curve changes into rhomboidal shaped loading curves, and the oil sample undergoes a sequence of mechanical processes which consist of an elastic loading, a saturation of the stress, and a final viscoplastic flow.

Though most previous investigations performed LAOStrain measurements on the structured fluids, fewer attention has been given to the nonlinear viscoelastic characteristics under stress-controlled large amplitude oscillatory shear (LAOStress). Wardhaugh and Boger (1991) studied the viscoelastic behavior of cooled waxy crude oils by oscillatory shear tests, and reported that when a low amplitude of shear stress was applied, the strain response of the tested oil

sample was perfectly in-phase with the applied shear stress, and this response was independent of the applied amplitude as well. While the applied stress amplitude is higher, the periodic strain waveforms deviate from sinusoid and present complex curves.

From the above reviews, it can be seen that the strain(stress)–time curves or Lissajous curves of waxy crude oils in LAOS measurements have been well presented. However, these complex curves, particularly under LAOStress, were not further analyzed and not been quantified as well. Furthermore, the LAOS characteristics of waxy crude oils at different frequencies still remain poorly understood.

These gaps in the literature have motivated the further research reported by Dimitriou et al. (2013). Extending some of the definitions for LAOStrain measurements by Ewoldt et al. (2008), Dimitriou et al. (2013) provided the corresponding LAOStress framework for analysis of the experimental data of yield stress fluids. A series of analytical methods such as Fourier transform rheology (Wilhelm et al. 1998), Chebyshev strain decomposition (Yu et al. 2009), Lissajous curves (Ewoldt et al. 2010), viscoelastic measures (Macias-Rodriguez et al. 2018) in the nonlinear regime, and Pipkin diagram analysis (Ewoldt et al. 2007) were included in the developed LAOStress framework.

The aim of this work is to demonstrate the nonlinear viscoelastic characteristics of waxy crude oils for the stress-controlled case with the aid of Dimitriou's LAOStress framework. In the present work, the LAOStress measurements for waxy crude oils were conducted at different stress amplitudes and angular frequencies to examine the effect of amplitude and frequency on the nonlinear oscillatory responses, respectively. Three oscillatory angular frequencies of 0.1, 1, and 10 rad/s were employed for the LAOStress measurements in this study, and the stress amplitudes were set as 1, 5, 10, 15, 20, 25, 30, 35, 40, 45, 50, 55, and 60 Pa. Then, the LAOStress framework proposed by Dimitriou et al. (2013) was adopted to quantitatively analyze the experimental results under LAOStress. Specifically, we introduced the following methods for the LAOStress data analysis to give a clear description for waxy crude oils: (1) applying Fourier transform rheology to indicate the nonlinearities; (2) using Chebyshev strain decomposition to characterize the nature of elastic and viscous nonlinearities; (3) analyzing Lissajous curves to interpret the mechanical transient process for the cyclic loading period; (4) calculating the energy dissipation to represent the total dissipation per cycle; (5) measuring viscoelastic parameters in the nonlinear regime to quantify the rich nonlinearities; (6) plotting the Pipkin diagram to represent the wealthy information of waxy crude oils. By the discussion and explanation of acquired LAOStress results for waxy crude oils, the accurate description for the dependence of the nonlinear

scenario on stress amplitude and angular frequency was finally concluded.

Experimental section

Materials

A waxy crude oil produced in China was used in this study. The rheological behaviors of waxy crude oils show strong dependencies on the thermal- and shear- history (Geri et al. 2017). To ensure better repeatability and comparability of the experimental results, the oil samples were first pretreated at 80 °C for 2 h and then allowed to cool naturally to the ambient temperature and kept for at least 48 h to reach a uniform state before being used (Sun and Zhang 2015; Andrade et al. 2015). The main physical properties of the pretreated crude oil and the corresponding experimental methods are listed in Table 1.

Rheological testing methods

The rheological tests in this work were performed by using a stress-controlled HAAKE Mars III rheometer (Thermo Fisher Scientific, Inc., Germany). All tests were conducted by a coaxial cylinder sensor system with rough surfaces (Z38 TiP) to minimum wall slip (Lopes-da-Silva and Coutinho 2007; Paso et al. 2009; Andrade et al. 2015; Japper-Jaafar et al. 2015).

The test procedure is as follows. The pretreated oil sample and the geometry were heated to 50 °C and held at that temperature for 30 min. The sample was then loaded into the rheometer and kept isothermally at 50 °C for 10 min, and then, it was statically cooled to the testing temperature at a constant cooling rate of 0.5 °C/min. Rheological measurements were performed after the oil sample was isothermally held at the testing temperature for 90 min to let the wax crystal structure fully develop. The test temperatures (11 °C) are just slightly lower than the gelation temperature (12.9 °C), and we believe that the wall slip is not significant for systems with such a low yield stress (Rønningsen 1992).

Table 1 Physical properties of the studied waxy crude oil

Physical parameter	Value	Test method
Density at 20 °C (kg/m^3)	836.8	ISO 3675-1998
WAT (°C)	25.8	Differential scanning calorimetry
Pour point (°C)	15.0	ASTM D5853-17
Gelation temperature (°C)	12.9	Dynamic rheological measurement
Wax content (wt %)	13.9	Differential scanning calorimetry
Resins (wt %)	5.5	ASTM D4124-09
Asphaltenes (wt %)	2.4	ASTM D4124-09

During the cooling and isothermal process, the SAOS measurement was carried out to track the temporal information of viscoelastic parameters with temperature and aging (Coutinho et al. 2003; Visintin et al. 2005; Lopes-da-Silva and Coutinho 2007) time. In this study, a strain amplitude of 0.001 and a constant frequency of 10 rad/s were adopted to ensure that the measurement was carried out within the linear viscoelastic regime. Figure 1 shows the variations in G' and G''. It can be seen that after isothermal aging for 90 min, both G' and G'' become virtually constant, meaning that the gel structure has fully developed and the oil sample has been ready for the subsequent rheological measurements.

Results and discussion

Oscillatory stress sweep

Oscillatory stress sweeps were first conducted starting from the stress amplitude σ_0 of 0 to 60 Pa to investigate the progressive transition from linear to nonlinear rheological responses of waxy crude oils. Three oscillatory angular frequencies ω of 0.1, 1, and 10 rad/s were used in the experiment to understand the effect of ω on the nonlinear responses. Figure 2 shows the dynamic moduli, G' and G'', as a function of σ_0. When σ_0 is relatively low, both the values of G' and G'' are virtually constant and the waxy gels behave a linear viscoelastic response. As the frequency increases, G' slightly increases within the linear viscoelastic region, consistent with the findings in the previous work we published on Journal of Rheology (Liu et al. 2018). Furthermore, Kané et al. (2004) also obtained the similar results in the frequency spectrum of waxy crude oils. Similar trends were also observed in other colloidal system (Derec et al. 2003; Purnomo et al. 2006; Ten Brinke et al. 2007; Koumakis and
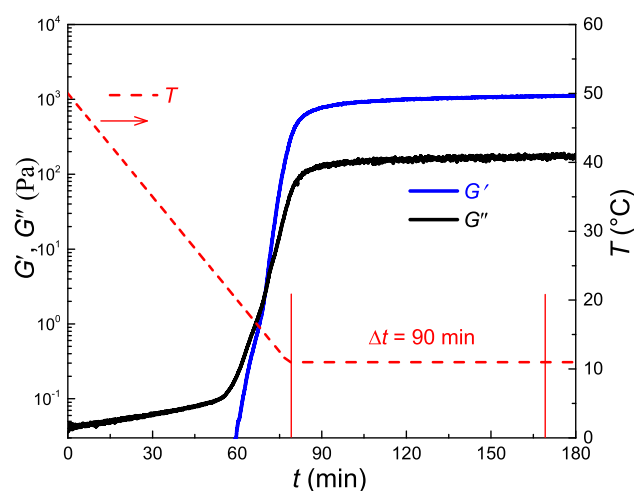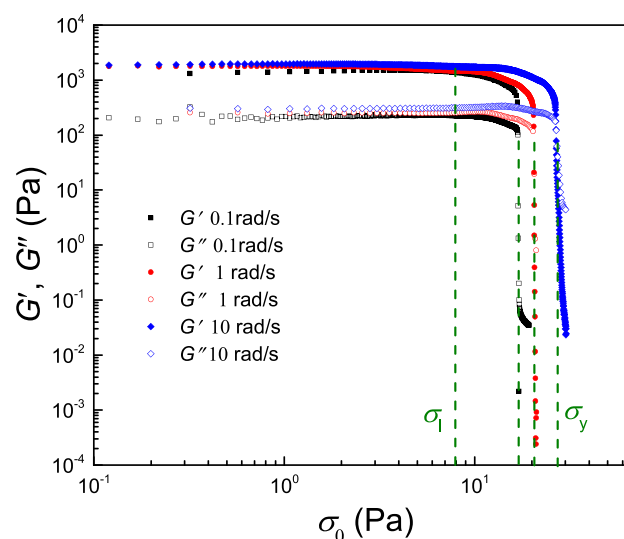
Fig. 2 Oscillatory stress sweeps at 0.1, 1, and 10 rad/s for gelled waxy crude oils formed at 11 °C

Petekidis 2011). For all the frequencies examined here, when σ_0 surpasses the limiting value of approximately 8 Pa (the critical linear stress σ_l), G' and G'' start to decrease gradually with increasing σ_0, implying that the samples start to evolve toward the nonlinear viscoelastic response (Hyun et al. 2011). It should be noted that a broader stress zone can be seen in this nonlinear process when using a higher ω, indicating a more gradual yielding. Further increase in σ_0 to a specific value (the yield stress σ_y) leads to the sharp drops of G' and G'', meaning the fracture of the waxy network. The values of σ_y for 0.1, 1 and 10 rad/s can then be determined to be 17, 21, and 27 Pa, respectively, and thus, a higher imposed ω would cause a higher σ_y. This finding has been also observed experimentally in other studies on waxy oil systems (Chang et al. 1998; Li et al. 2009; Tarcha et al. 2015; Liu et al. 2018).

Fourier transform and Chebyshev strain decomposition

Fourier transform analysis

Fourier transform (FT) rheology is a common method to quantify the LAOS tests (Carotenuto et al. 2008). The approach developed by Dimitriou et al. (2013) was used for the Fourier transform analysis of the LAOStress data in this study. Suppose that a sinusoidal stress is imposed on the gelled waxy crude oils, and the convention to a cosine wave for the imposed stress is adopted to simplify the expressions used to determine the Chebyshev coefficients in the subsequent sections:

$$\sigma(t) = \sigma_0 \cos \omega t \tag{1}$$

Fig. 1 Temporal variation in G', G'' and temperature during the cooling and isothermal aging processes

Via a complex Fourier transformation, the strain response $\gamma(t;\sigma_0;\omega)$ can then be represented by a Fourier series, written in terms of the harmonic amplitude I_n and the phase angle φ_n of all different harmonic contributions as follows:

$$\gamma(t;\sigma_0;\omega) = \sum_{n\,\text{odd}} I_n \cos\left(n\omega t + \varphi_n\right) \tag{2}$$

We consider that only odd harmonics were included in this equation, and the conditions (the presence of transient responses, dynamic wall slip and secondary flows) resulting in the even-harmonic terms were not considered in this study (Atalık and Keunings 2004). Thus, Fourier transformation for the temporal variations in strain can result in the distinct peaks in the Fourier rheology spectrum at the odd multiples of the fundamental frequency, i.e., $\omega, 3\omega, 5\omega\cdots\cdots$ In order to avoid non-systematic calibration errors, the absolute intensity of the nth harmonic I_n can be normalized by the intensity at the fundamental frequency shown in Eq. (3), which changes I_n to the relative intensity I_{n1}.

$$I_{n1} = \frac{I_n}{I_1} \tag{3}$$

For instance, Fig. 3 shows the normalized Fourier rheology spectra for the LAOStress data at $\omega=0.1\text{rad/s}$ and $\sigma_0=25\text{Pa}$. The main peak of the normalized Fourier rheology spectra exactly occurs at the position of odd multiples of ω and the signal values of I_{n1} decrease gradually as the harmonical number n increases.

In order to quantify the degree of the nonlinear response, we gave particular attention to the relative intensity of higher harmonic contributions, and Fig. 4 depicts the relative intensity of the third harmonic I_{31} for waxy crude oils as a function of σ_0.

It can be found that for the three oscillatory angular frequencies, the values of I_{31} firstly increase following an exponential relationship with a slope of 0.003 and reach the maximum, and then decrease with increasing σ_0. It must be mentioned that the point corresponding to the maximum of I_{31} can be identified as the yield point, and the stress at the maximum point is the yield stress, which is consistent with the yield stress obtained in oscillatory stress sweep tests for the three used angular frequencies in "Oscillatory stress sweep" section. Furthermore, a larger value of I_{31} can be observed when applying a lower ω.

Chebyshev strain decomposition

In this section, we used the method of Chebyshev strain decomposition to separately characterize the nature of elastic and viscous nonlinearities.

a. Chebyshev compliance coefficients and fluidity coefficients

Just as the following forms, the Fourier series of strain response $\gamma(t;\sigma_0;\omega)$ in Eq. (2) can also be decomposed into a superposition of an apparent elastic strain γ' and apparent plastic strain γ'' to emphasize either the elastic or viscous scaling, respectively. A series of orthogonal Chebyshev polynomials of the first kind $T_n(x)$, where x is the scaled stress $x=\sigma(t)/\sigma_0$, were then selected to represent the elastic and viscous contributions to the measured strain response.

$$\gamma(t;\sigma_0,\omega) = \sum_{n\,\text{odd}} \left[J'_n(\omega,\sigma_0)\sigma_0\cos n\omega t + J''_n(\omega,\sigma_0)\sigma_0\sin n\omega t\right] \tag{4}$$
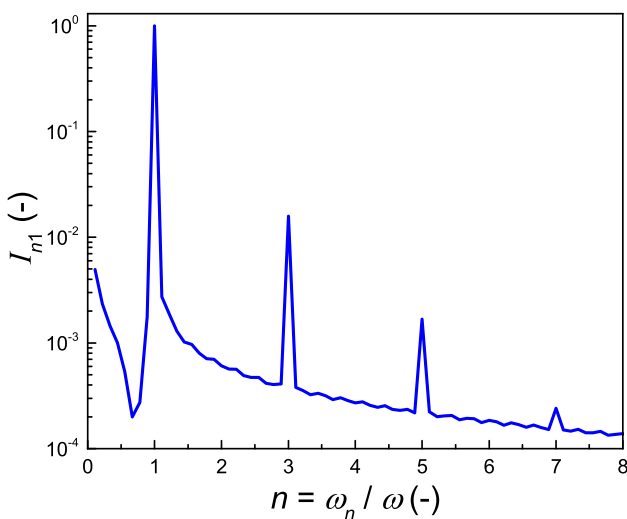

Fig. 3 Normalized Fourier spectra of the steady oscillatory strain signal for gelled waxy crude oils formed at 11 °C under oscillatory stress at $\omega=0.1\text{rad/s}$ and $\sigma_0=25\text{Pa}$
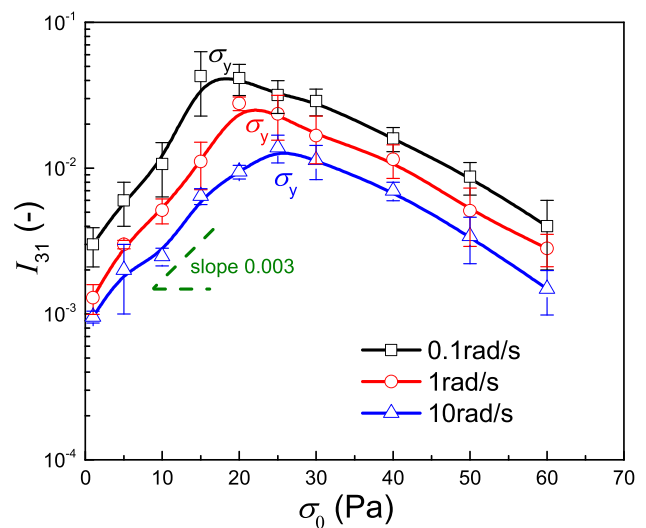

Fig. 4 Relative intensity of the third harmonic I_{31} as a function of applied stress amplitude σ_0 under the frequency of 0.1, 1, and 10 rad/s for gelled waxy crude oils formed at 11 °C

$$\gamma'(t) = \sigma_0 \sum_{n \text{ odd}} [J_n'(\omega, \sigma_0) \cos n\omega t] = \sigma_0 \sum_{n \text{ odd}} [\underbrace{J_n'(\omega, \sigma_0)}_{c_n} T_n(x)] \tag{5}$$

$$\gamma''(t) = \sigma_0 \sum_{n \text{ odd}} [J_n''(\omega, \sigma_0) \sin n\omega t] \tag{6}$$

$$\dot{\gamma}''(t) = \sigma_0 \sum_{n \text{ odd}} [n\omega J_n''(\omega, \sigma_0) \cos n\omega t] = \sigma_0 \sum_{n \text{ odd}} [\underbrace{n\omega J_n''(\omega, \sigma_0)}_{f_n} T_n(x)] \tag{7}$$

where γ' is the apparent elastic strain; γ'' is the apparent plastic strain; $\dot{\gamma}''$ is the plastic strain rate, s^{-1}; J_n' and J_n'' are the nth-order harmonic Fourier coefficients, Pa^{-1}; T_n is the orthogonal Chebyshev polynomials, $T_n(cos\theta) = cosn\theta$; x is the scaled stress, $x = \sigma(t)/\sigma_0$; c_n is the Chebyshev compliance coefficients, Pa^{-1}; f_n is the Chebyshev fluidity coefficients, $[Pa \cdot s]^{-1}$.

The Chebyshev polynomials of the first kind are orthogonal over the domain $[-1, 1]$, and the $n=1, 3, 5$-order Chebyshev polynomials are given below.

$$T_1(x) = x \tag{8}$$

$$T_3(x) = 4x^3 - 3x \tag{9}$$

$$T_5(x) = 16x^5 - 20x^3 + 5x \tag{10}$$

From the above framework, we refer to $c_n(\omega, \sigma_0)$ as the Chebyshev compliance coefficients to signify the elastic properties, and $f_n(\omega, \sigma_0)$ as the Chebyshev fluidity coefficients to signify the viscous properties. As an example, Fig. 5 shows the obtained c_n (a) and f_n (b) for gelled waxy crude oils under the oscillatory frequency of 0.1 rad/s and stress amplitude of 20 Pa. The third-order Chebyshev coefficients c_3 and f_3 are the leading order of nonlinearity and can provide the physical insight into the deviation from linear viscoelasticity (Ptaszek 2015). The LAOStress framework means that $c_3 > 0$ corresponds to intracycle stress softening

of the $\gamma' \sim \sigma$ curve, whereas $c_3 < 0$ indicates stress stiffening. Similarly, a positive value for f_3 represents stress thinning of the $\dot{\gamma}'' \sim \sigma$ curve, and $f_3 < 0$ describes stress thickening in the viscosity (Dimitriou et al. 2013).

b. Scaled third-order Chebyshev coefficients

It is common to use the scaled third-order Chebyshev coefficients c_3/c_1 and f_3/f_1 to indicate the nature of the elastic and viscous nonlinearities, respectively. Since c_1 and f_1 are always positive, the signs of c_3/c_1 and f_3/f_1 have equivalent interpretations to c_3 and f_3, respectively. The relation of c_3/c_1 and f_3/f_1 with I_{31} can be well expressed as follows:

$$c_3/c_1 = I_{31} \cdot \cos\varphi_3/\cos\varphi_1 \tag{11}$$

$$f_3/f_1 = I_{31} \cdot \sin\varphi_3/\sin\varphi_1 \tag{12}$$

The variations in c_3/c_1 and f_3/f_1 with σ_0 for waxy crude oils are shown in Fig. 6a and b, respectively. At these frequencies, the values of c_3/c_1 are always negative, whereas the f_3/f_1 coefficients are always positive. This indicates that the waxy crude oils exhibit stress stiffening for the $\gamma' \sim \sigma$ curve and stress thinning for the $\dot{\gamma}'' \sim \sigma$ curve. From Fig. 6, it can also be observed that both c_3/c_1 and f_3/f_1 grow initially when σ_0 is relatively low. As σ_0 increases to approximately σ_y, both c_3/c_1 and f_3/f_1 reach the maximum and then start to decrease rapidly with the increase in σ_0, suggesting the degradation of

Fig. 5 Elastic Chebyshev harmonics (**a**) and viscous Chebyshev harmonics (**b**) for gelled waxy crude oils formed at 11 °C under oscillatory stress at $\omega = 0.1$rad/s and $\sigma_0 = 20$Pa
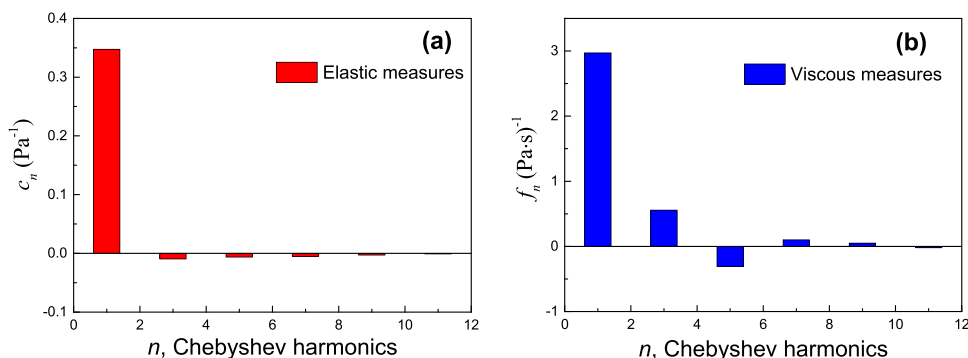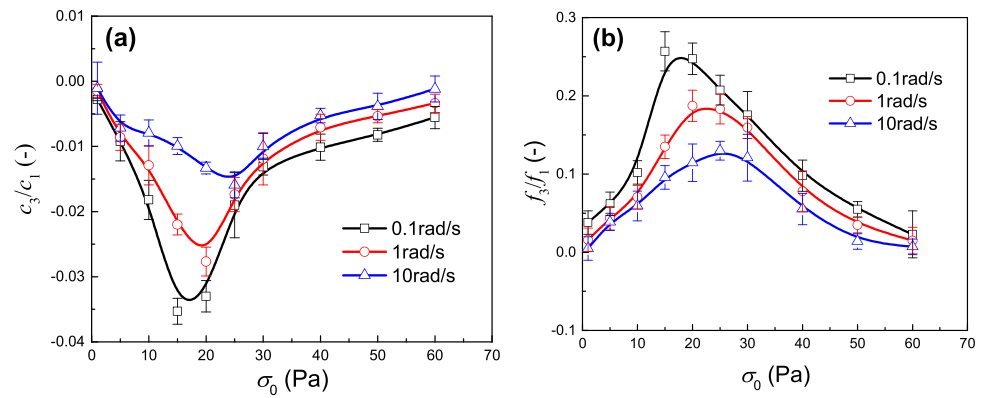
Fig. 6 Dependence of the scaled third-order elastic Chebyshev coefficient c_3/c_1 (**a**) and viscous Chebyshev coefficient f_3/f_1 (**b**) on the stress amplitude σ_0 under the frequency of 0.1, 1, and 10 rad/s for gelled waxy crude oils formed at 11 °C

the nonlinear nature. Moreover, both the values of c_3/c_1 and f_3/f_1 are found to be larger when using a lower ω.

Discussion of the physical meaning

The above experimental observations indicate that the nonlinear degree of the interlocking waxy network can be gradually strengthened within a certain range of σ_0 and subsequently weakened as σ_0 increases surpassing σ_y.

Note that a low value of I_{31} can be captured in the linear viscoelastic region, which was also observed in the report of Hyun et al. (2011). Based on the findings from the previous studies of Dimitriou et al. (2013), we believe that the gelled waxy crude oils can show weakly nonzero viscous dissipation behaviors within an "elastically" dominated region at stresses below σ_1. Furthermore, only 80%, not 100%, of the total deformation within the linear viscoelastic region was found to be recoverable using creep-recovery experiments in the previous work we published for waxy crude oils (Liu et al. 2018). All these can provide support for the occurrence of a low value of I_{31} in the linear viscoelastic region. However, such low I_{31} didn't mean that waxy oil systems show a nonlinear response at stress lower than σ_1 and its linear viscoelasticity for such I_{31} instead.

According to the classification by Hyun et al. (2011), the materials of gelled waxy crude oils can be regarded as soft gel state, exhibiting a local maximum for I_{31}. Similar trends have been also observed in other soft colloidal systems, such as rigid polymer dispersions (Kallus et al. 2001), highly concentrated suspensions of PMMA particles (Heymann et al. 2002), and highly loaded carbon black filled rubber compounds (Leblanc 2008). Different from the carbopol sample, the network formed by interconnected wax crystals in oils is tight and brittle, forming the rigid status for the micellar aggregates, which is usually the case for many soft gels. After the waxy network structure yields and fractures, the nonlinearity of gelled oils becomes weak.

Finally, the waxy crude oils show more striking characteristics of both the elastic and viscous nonlinearities at lower ω, meaning that a longer characteristic time could favor the degree of the nonlinear response.

Lissajous curves analysis

The mechanical transient characteristics during LAOS loading period were then analyzed by using Lissajous curves tracing. The obtained periodic strain response at steady state from LAOS was used for the data processing. In order to eliminate the problem of noise amplification, we use the odd, integer Fourier coefficients in Eq. (2) to reconstruct the strain time data. The smoothed total strain signals after discrete comb filter reconstruction were further used for Lissajous curves analysis. The Lissajous curves include the elastic Lissajous curves and viscous Lissajous curves (Läuger and Stettin 2010). The elastic Lissajous curves in LAOStress refer to the oscillatory response curves of $\gamma(t)$ vs. $\sigma(t)$, and the viscous Lissajous curves denote the curves of $\dot{\gamma}(t)$ vs. $\sigma(t)$.

Stress amplitude dependence

To investigate the dependence of Lissajous curves on σ_0, we plotted the Lissajous curves at three applied stress amplitudes of 5, 15, and 30 Pa for the region of linear viscoelasticity, nonlinear viscoelasticity, and post-yielding, respectively. Under the frequency of 1 rad/s, the elastic Lissajous curves for waxy crude oils at these three stress amplitudes are displayed in Fig. 7a, b and c, and the viscous Lissajous curves are displayed in Fig. 7d, e and f. While the applied σ_0 (5 Pa) is in the linear viscoelastic region, the elastic Lissajous curve appears as an oblate elliptic loop, and the shape of viscous Lissajous curve appears as a circular elliptic shape. As σ_0 increases to 15 Pa, the corresponding strain signal output has non-sinusoidal shape for a sinusoidal stress input, and both the elastic and viscous Lissajous curves are distorted from the perfect elliptic forms, signifying the transition from the linear to nonlinear viscoelastic response. At a larger amplitude σ_0=30 Pa, the elastic Lissajous curve becomes almost
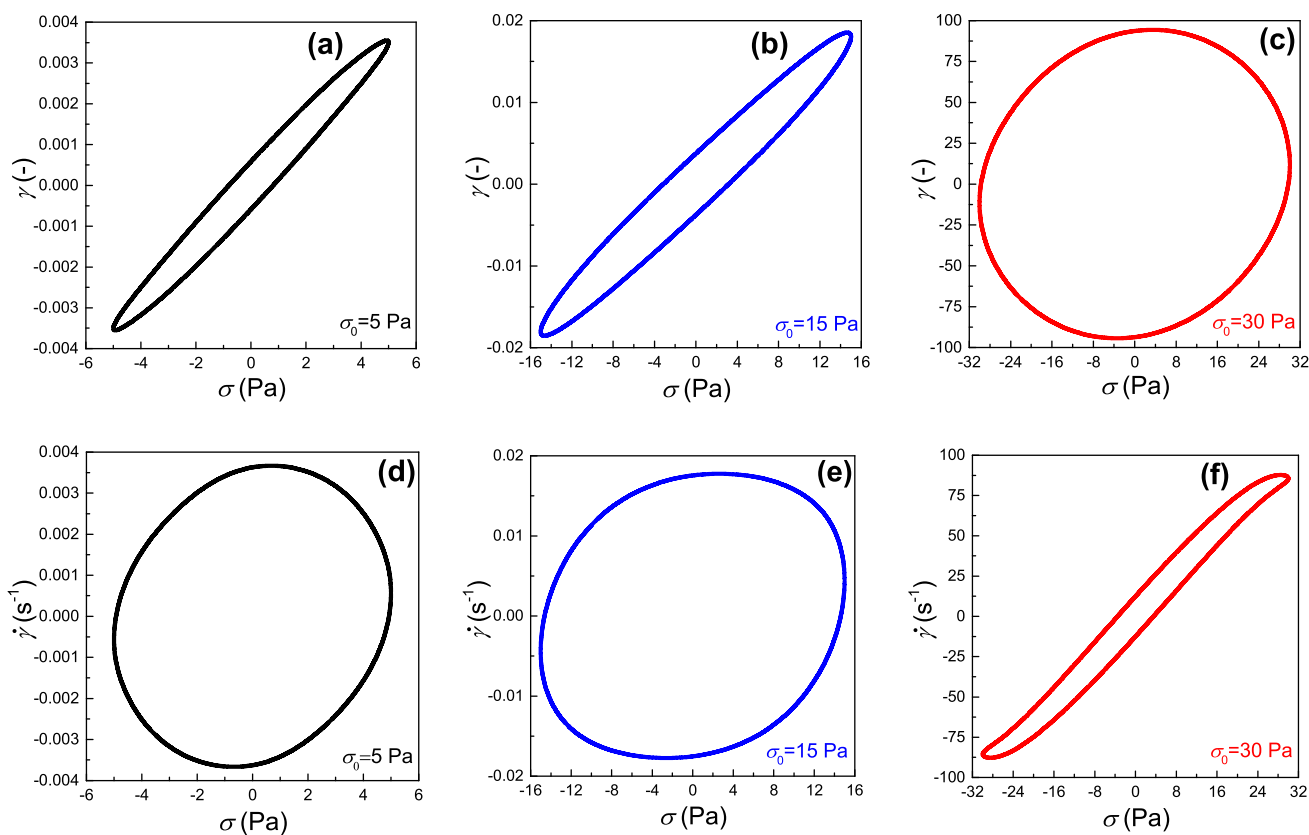
Fig. 7 Elastic Lissajous curves of $\gamma(t)$vs$\sigma(t)$ (**a**, **b**, and **c**) and viscous Lissajous curves of $\dot{\gamma}(t)$vs$\sigma(t)$ (**d**, **e**, and **f**) at three stress amplitudes of 5, 15 and 30 Pa under the oscillatory frequency of 1 rad/s for gelled waxy crude oils formed at 11 °C

a rounded parallelogram, and the viscous Lissajous curve at this σ_0 becomes a distorted and oblate lozenge shape.

More insights into the information of Lissajous curves can be gained when plotting the Lissajous curves of different stress amplitudes in the same picture. Figure 8a shows these elastic Lissajous curves for waxy crude oils under the same frequency of 1 rad/s, and Fig. 8b shows the viscous Lissajous curves. It can be observed that with the increase in the imposed σ_0, both the

elastic and viscous Lissajous curves rotate counterclockwise, and the area enclosed within the Lissajous curves increases significantly, reflecting the gradual decay of waxy structure.

Frequency dependence

In order to clearly present the variations in Lissajous curves with oscillatory angular frequency ω, the Lissajous curves

Fig. 8 Elastic Lissajous curves of $\gamma(t)$vs$\sigma(t)$ (**a**) and viscous Lissajous curves of $\dot{\gamma}(t)$vs$\sigma(t)$ (**b**) at different stress amplitudes under the oscillatory frequency of 1 rad/s for gelled waxy crude oils formed at 11 °C
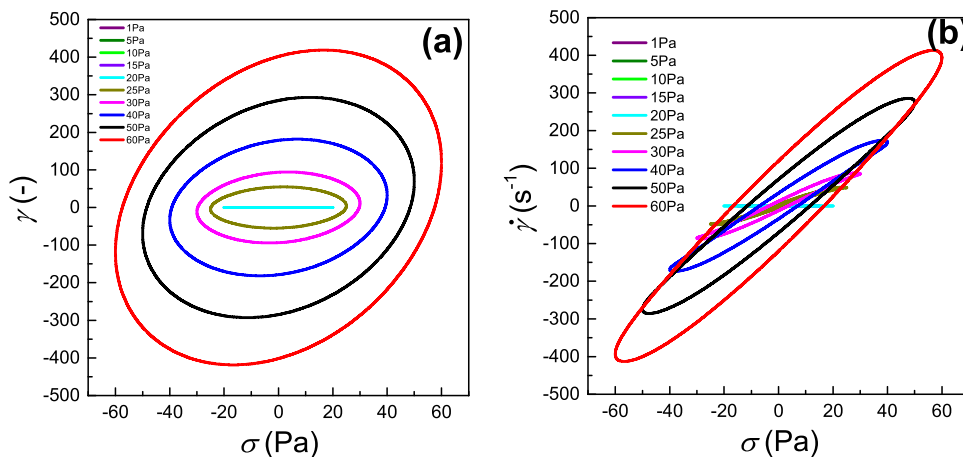
at different frequencies of 0.1, 1, and 10 rad/s were plotted in the same picture. The plotted elastic Lissajous curves for waxy crude oils under the applied σ_0 of 5, 15, and 30 Pa are shown in Fig. 9a, b and c, respectively, and the viscous Lissajous curves are shown in Fig. 9d, e and f. It can be found that with the increase in ω, the elastic Lissajous curves rotate clockwise, and both the induced strain amplitude γ_0 and the area enclosed within the Lissajous curves monotonically decrease. As to the viscous Lissajous curves, the induced maximum shear rate $\dot{\gamma}_0$ increases with increasing ω before yielding at σ_0 of 5 Pa and 15 Pa. However, the values of $\dot{\gamma}_0$ show an opposite trend after the structural yielding at σ_0 of 30 Pa, decreasing with the increase in ω. To demonstrate the curve information more clearly and precisely, the rotation characteristics for the viscous Lissajous curves at different frequencies are discussed in "Elastic strain and plastic strain rate" section.

Discussion of the physical meaning

The waxy structure can be gradually destroyed with the increase in imposed σ_0, and large increase for the shear rate and shear strain can be observed after the structural yielding. In addition, a higher structural strength for the interlocking waxy network can be measured under a higher ω.

Elastic strain and plastic strain rate

In "Chebyshev strain decomposition" section, the strain response $\gamma(t; \sigma_0; \omega)$ in LAOStress can be decomposed into a superposition of elastic and viscous scaling by Chebyshev strain decomposition, and the scaled third-order Chebyshev coefficients were used to characterize the nature of nonlinearities. In this section, we calculated and presented the measures of elastic strain γ' and plastic strain rate $\dot{\gamma}''$ to further get more information of nonlinear viscoelasticity characteristics in the elastic and viscous Lissajous curves, respectively. Both the calculation of γ' and $\dot{\gamma}''$ can also be related with the symmetry method (Ewoldt et al. 2008), and both the values of them are single-valued functions of σ over one cycle of oscillation, which can be written as the following equations:

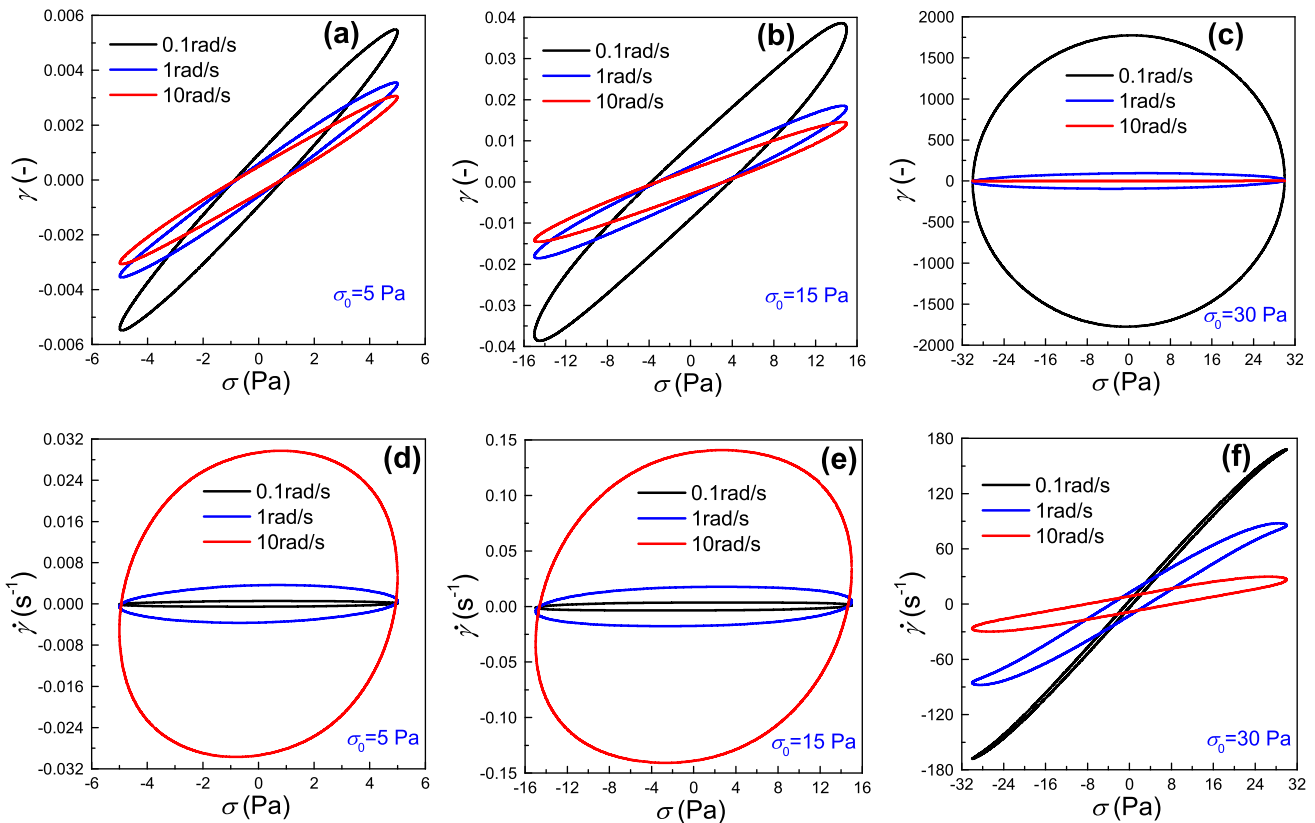$$\gamma'(t) = \frac{\gamma(\sigma, \dot{\gamma}) - \gamma(-\sigma, \dot{\gamma})}{2} \qquad (13)$$

Fig. 9 Elastic Lissajous curves of $\gamma(t)$vs$\sigma(t)$ (**a**, **b**, and **c**) and viscous Lissajous curves of $\dot{\gamma}(t)$vs$\sigma(t)$ (**d**, **e**, and **f**) at different frequencies under the stress amplitude of 5, 15, and 30 Pa for gelled waxy crude oils formed at 11 °C

$$\dot{\gamma}''(t) = \frac{\dot{\gamma}(\sigma, \gamma) - \dot{\gamma}(-\sigma, \gamma)}{2} \quad (14)$$

Taking the LAOStress data under the imposed σ_0 of 20 Pa and ω of 1 rad/s as an example, the geometrical interpretations of γ' (a) and $\dot{\gamma}''$ (b) in Lissajous curves for waxy crude oils are observed in Fig. 10. It is clear that both γ' and $\dot{\gamma}''$ depend on the imposed σ only, and γ' and $\dot{\gamma}''$ curves are the centerlines of the elastic Lissajous curve and viscous Lissajous curve, respectively. Thus, the rotation characteristics of the elastic and viscous Lissajous curves can also be reflected by that of the γ' and $\dot{\gamma}''$ curves, respectively.

Stress amplitude dependence

We plotted the γ' and $\dot{\gamma}''$ curves at different stress amplitudes in the same picture to further get the evolution information of γ' and $\dot{\gamma}''$ with imposed σ_0, respectively. Figure 11a, b and c shows the plotted γ' curves for waxy crude oils under the applied ω of 0.1, 1 and 10 rad/s, respectively, and Fig. 11d, e and f shows the $\dot{\gamma}''$ curves. It can be seen that with increasing σ_0, both the γ' and $\dot{\gamma}''$ curves rotate counterclockwise, and both the induced elastic strain amplitude γ_0' and the induced maximum plastic strain rate $\dot{\gamma}_0''$ gradually increase.

Frequency dependence

The dependence of γ' and $\dot{\gamma}''$ on ω can be investigated when plotting the γ' and $\dot{\gamma}''$ curves at different oscillatory frequencies of 0.1, 1 and 10 rad/s in the same picture. The plotted γ' curves for waxy crude oils under the applied σ_0 of 5, 15, and 30 Pa are illustrated in Fig. 12a, b and c, respectively, and the $\dot{\gamma}''$ curves are illustrated in Fig. 12d, e and f. From Fig. 12a, b and c, the γ' curves and the induced γ_0' were found to rotate clockwise and monotonically decrease with the increase in applied ω, respectively. As shown in Fig. 12d and e, when the imposed σ_0 (5 and 15 Pa) is lower than σ_y, the $\dot{\gamma}''$ curves rotate counterclockwise, and the induced $\dot{\gamma}_0''$ gradually

increases with the increase in applied ω. However, compared with the observations before yielding, Fig. 12f (σ_0=30 Pa) shows that the $\dot{\gamma}''$ curves together with the induced $\dot{\gamma}_0''$ exhibit the opposite trends after yielding. That is the $\dot{\gamma}''$ curves rotating clockwise and the induced $\dot{\gamma}_0''$ decreasing with increasing ω.

Discussion of the physical meaning

These observations suggest that the flowability of gelled waxy crude oils can be significantly enhanced with increasing σ_0 through sustained shear. Furthermore, a lower applied ω is more favorable for the structural nonlinear destruction of waxy network.

Energy dissipation characteristic analysis

Through the mathematical method, the dissipated energy E_d in a full oscillation cycle period can be determined by using the following integral of Eq. (15). Geometrically, E_d can be visualized and indicated by the area enclosed within the elastic Lissajous curves (Ewoldt et al. 2010; Yang et al. 2015).

$$E_d = \int_0^{2\pi/\omega} \sigma\dot{\gamma}\,dt = \oint \gamma(t)\,d\sigma \quad (15)$$

Figure 13 shows the evolutions of E_d with the imposed σ_0 for waxy crude oils under ω of 0.1, 1, and 10 rad/s. It is obvious that E_d increases monotonically with the increase in σ_0, indicating that a larger imposed σ_0 dissipates more energy for waxy gel under the same ω. The reasons may be interpreted by analyzing the two calculated factors affecting the energy dissipation during the full oscillation cycle period, namely the applied oscillatory stress and generated oscillatory strain. A higher oscillatory stress causes a higher oscillatory strain due to induced structural degradation, and thus, E_d continues to show a high value with increasing

Fig. 10 Elastic strain γ' in elastic Lissajous curve (**a**) and the plastic strain rate $\dot{\gamma}''$ in viscous Lissajous curve (**b**) during an oscillation cycle for gelled waxy crude oils formed at 11 °C under oscillatory stress at σ_0=20Pa and ω=1rad/s
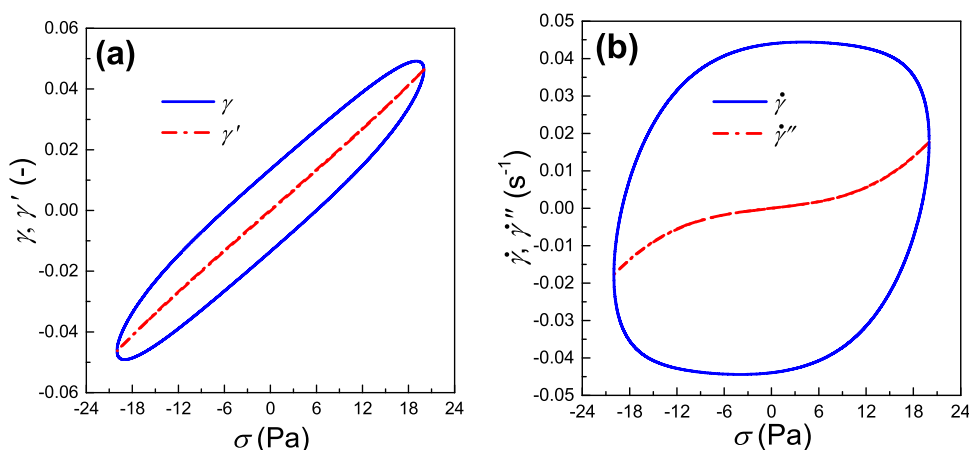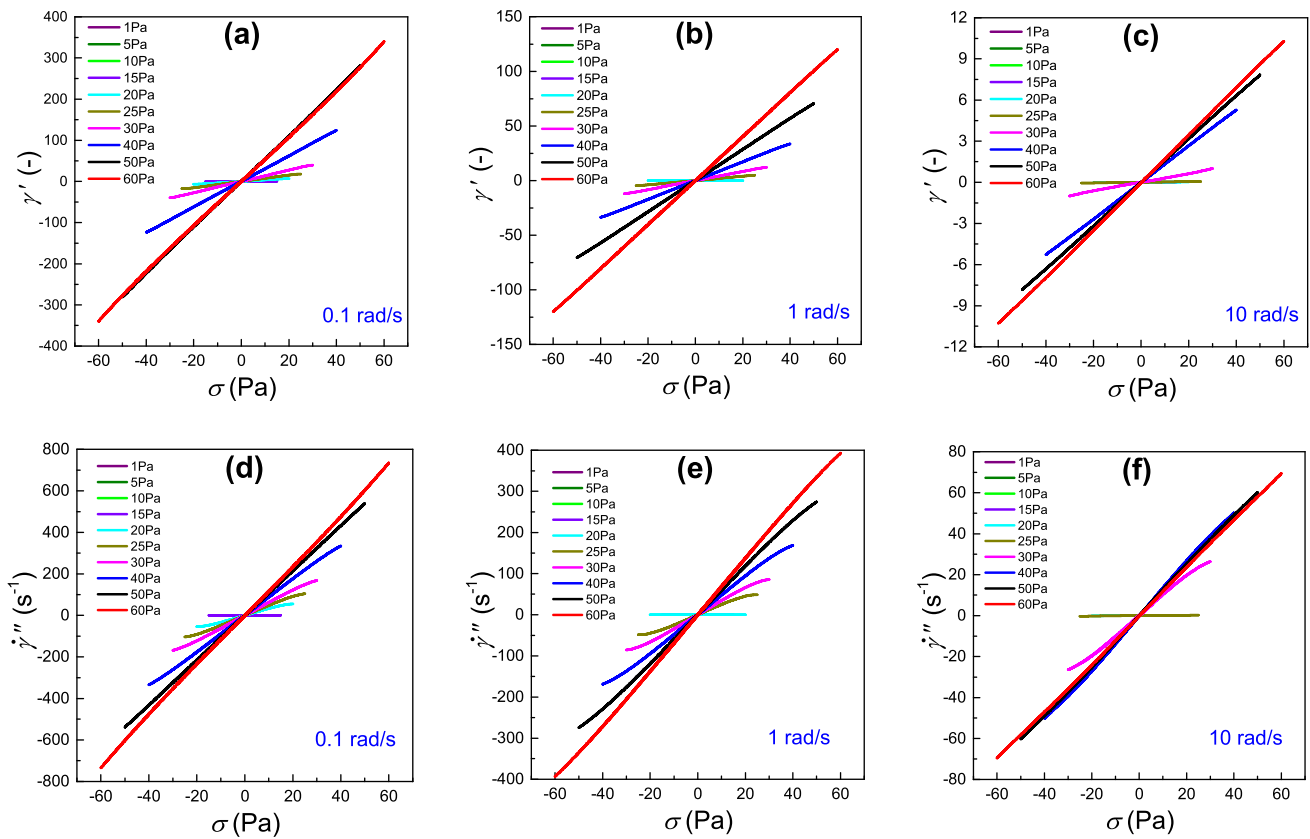
Fig. 11 Evolutions of elastic strain γ' with shear stress σ (**a**, **b**, and **c**) and plastic strain rate $\dot{\gamma}''$ with shear stress σ (**d**, **e**, and **f**) at different stress amplitudes under the oscillatory frequency of 0.1, 1, and 10 rad/s for gelled waxy crude oils formed at 11 °C

σ_0. Another observation we made from Fig. 13 is that the obtained E_d has a higher value when using a lower ω, suggesting that a significant energy dissipation characteristic for waxy crude oils can be captured at lower ω.

Viscoelastic measures analysis

Though Fourier transform analysis discussed above, the periodic strain response after Fourier transformation will include only the first harmonic contributions in the linear viscoelastic region (Ewoldt et al. 2010; Wang et al. 2011; Dimitriou et al. 2013). Therefore, the first harmonic coefficients J_1' and J_1'' can be used as the measures of the linear viscoelastic response. However, the nonlinear data signals at larger σ_0 lead to the appearance of higher harmonic contributions, and thus, J_1' and J_1'' fail to accurately describe the rich nonlinearities under large amplitude for the raw data signal. Based on the Fourier series analysis of elastic and viscous scaling shown in Eq. (4), the framework of Dimitriou et al. (2013) was adopted to quantify the nonlinear viscoelasticity of waxy crude oils, and the defined new nonlinear variables were expressed in Eq. (16) to Eq. (19). The defined nonlinear elastic measures include the minimum stress compliance J_M'

and large stress compliance J_L', and the nonlinear viscous measures include the minimum stress fluidity ϕ_M' and large stress fluidity ϕ_L'. Note that both the values of J_M' and J_L' are equivalent to J_1' in the linear regime, and ϕ_M' and ϕ_L' reduce to $\phi' = \omega J_1''$ for a linear viscoelastic response as well.

$$J_M' = \left.\frac{d\gamma}{d\sigma}\right|_{\sigma=0} = \sum_{n\,\text{odd}} (-1)^{(n-1)/2} n J_n' = \sum_{n\,\text{odd}} (-1)^{(n-1)/2} n c_n \tag{16}$$

$$J_L' = \left.\frac{\gamma}{\sigma}\right|_{\sigma=\sigma_0} = \sum_{n\,\text{odd}} J_n' = \sum_{n\,\text{odd}} c_n \tag{17}$$

$$\phi_M' = \left.\frac{d\dot{\gamma}}{d\sigma}\right|_{\sigma=0} = \sum_{n\,\text{odd}} (-1)^{(n-1)/2} n^2 \omega J_n'' = \sum_{n\,\text{odd}} (-1)^{(n-1)/2} n f_n \tag{18}$$

$$\phi_L' = \left.\frac{\dot{\gamma}}{\sigma}\right|_{\sigma=\sigma_0} = \sum_{n\,\text{odd}} n \omega J_n'' = \sum_{n\,\text{odd}} f_n \tag{19}$$

The calculated nonlinear elastic measures (J_M' and J_L') and nonlinear viscous measures (ϕ_M' and ϕ_L') are shown in Fig. 14a and b, respectively. It can be seen that with the
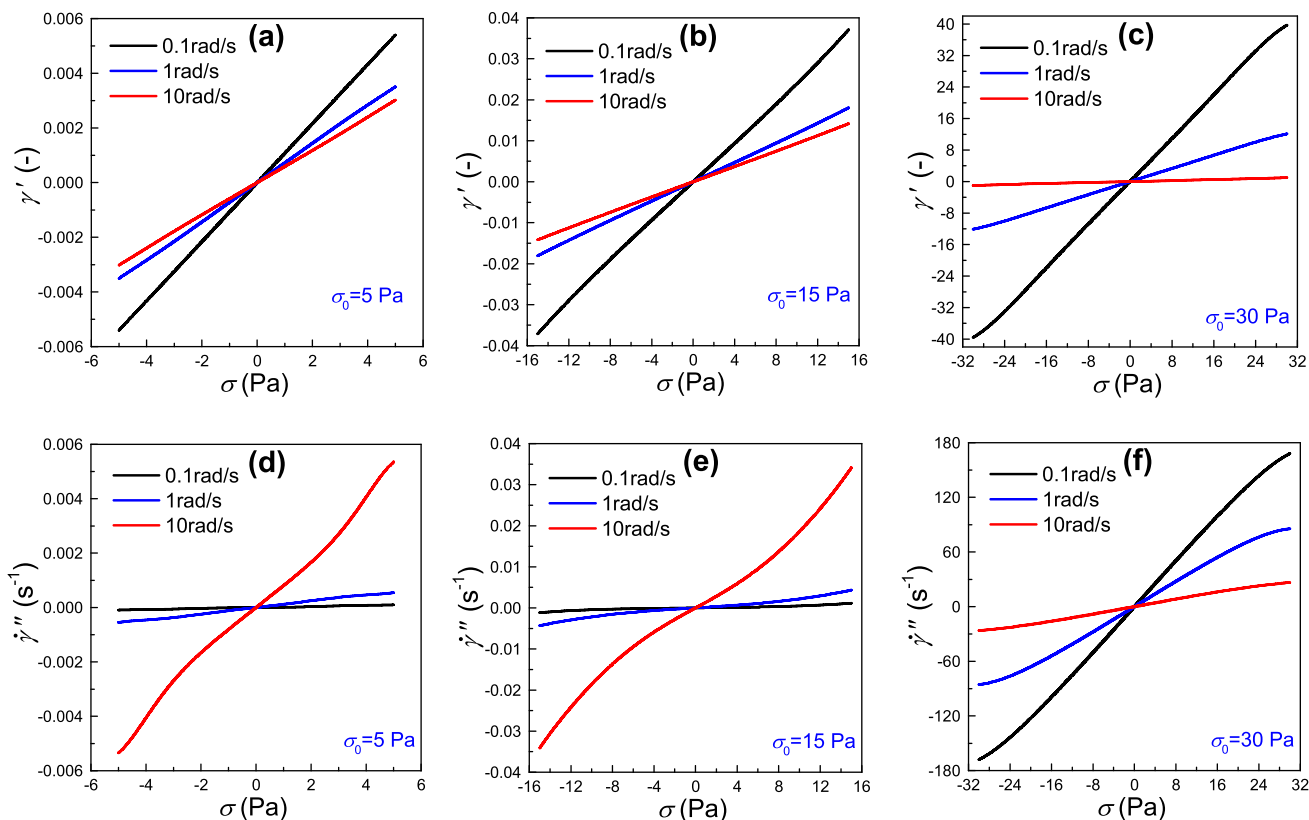
Fig. 12 Evolutions of elastic strain γ' with shear stress σ (**a**, **b**, and **c**) and plastic strain rate $\dot{\gamma}''$ with shear stress σ (**d**, **e**, and **f**) at different frequencies under the stress amplitude of 5, 15, and 30 Pa for gelled waxy crude oils formed at 11 °C
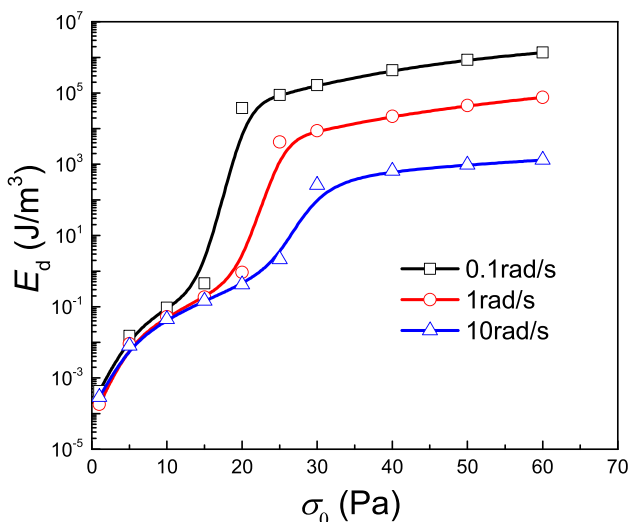

Fig. 13 Dependence of the energy dissipation per oscillation cycle E_d on the stress amplitude σ_0 under the oscillatory frequency of 0.1, 1, and 10 rad/s for gelled waxy crude oils formed at 11 °C

increase in imposed σ_0, both the elastic and viscous measures gradually increase when σ_0 is relatively low for all the three frequencies, and these measures dramatically increase

around the yield point, and then, the increase in viscoelastic measures slows down after the waxy oils yield. Furthermore, all the obtained viscoelastic measures are found to be larger when using a lower applied ω, even in the linear region. The reason for the dependence is that the network structure formed by wax crystals is linear viscoelastic, not purely elastic, containing weakly nonzero viscous dissipation in this linear rheological response region. All these observations indicate that more significant flowable characteristics for waxy oil systems can be gained under a higher imposed σ_0 and a lower ω. The last finding we can get from Fig. 14 is that the values of J'_M are larger than J'_L, while the values of ϕ'_M are smaller than ϕ'_L at the given σ_0 and ω for waxy crude oils. According to the research of Dimitriou et al. (2013), these indicate the stress stiffening ($J'_M > J'_L$) and stress thinning ($\phi'_M < \phi'_L$) behaviors for the studied system of crude oils, consistent with the findings of c_3 and f_3 by Chebyshev strain decomposition in "Chebyshev strain decomposition" section.

Pipkin diagram analysis

Pipkin diagram is an useful approach to summarize the rich viscoelastic characteristics of the studied material as a function of both imposed σ_0 and ω (Ewoldt et al. 2007; Stickel

Fig. 14 Dependence of the nonlinear elastic measures (minimum-stress compliance J'_M and large-stress compliance J'_L in **a**) and nonlinear viscous measures (minimum-stress fluidity ϕ'_M and large-stress fluidity ϕ'_L in **b**) on the stress amplitude σ_0 under the frequency of 0.1, 1, and 10 rad/s for gelled waxy crude oils formed at 11 °C
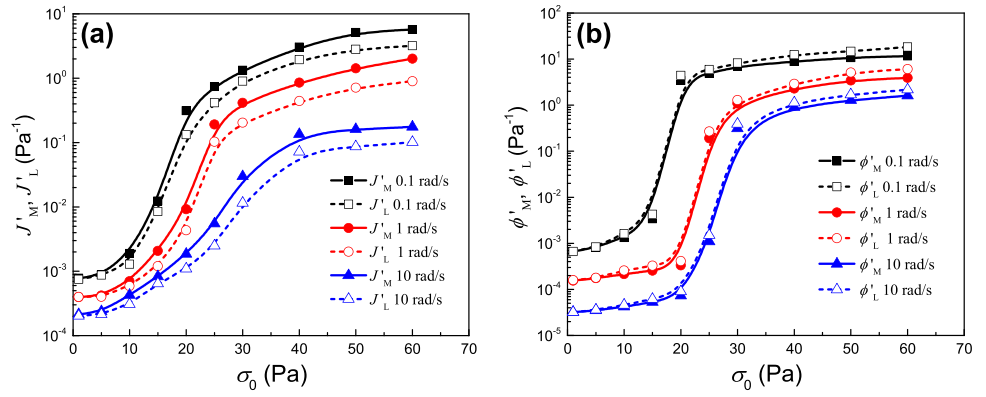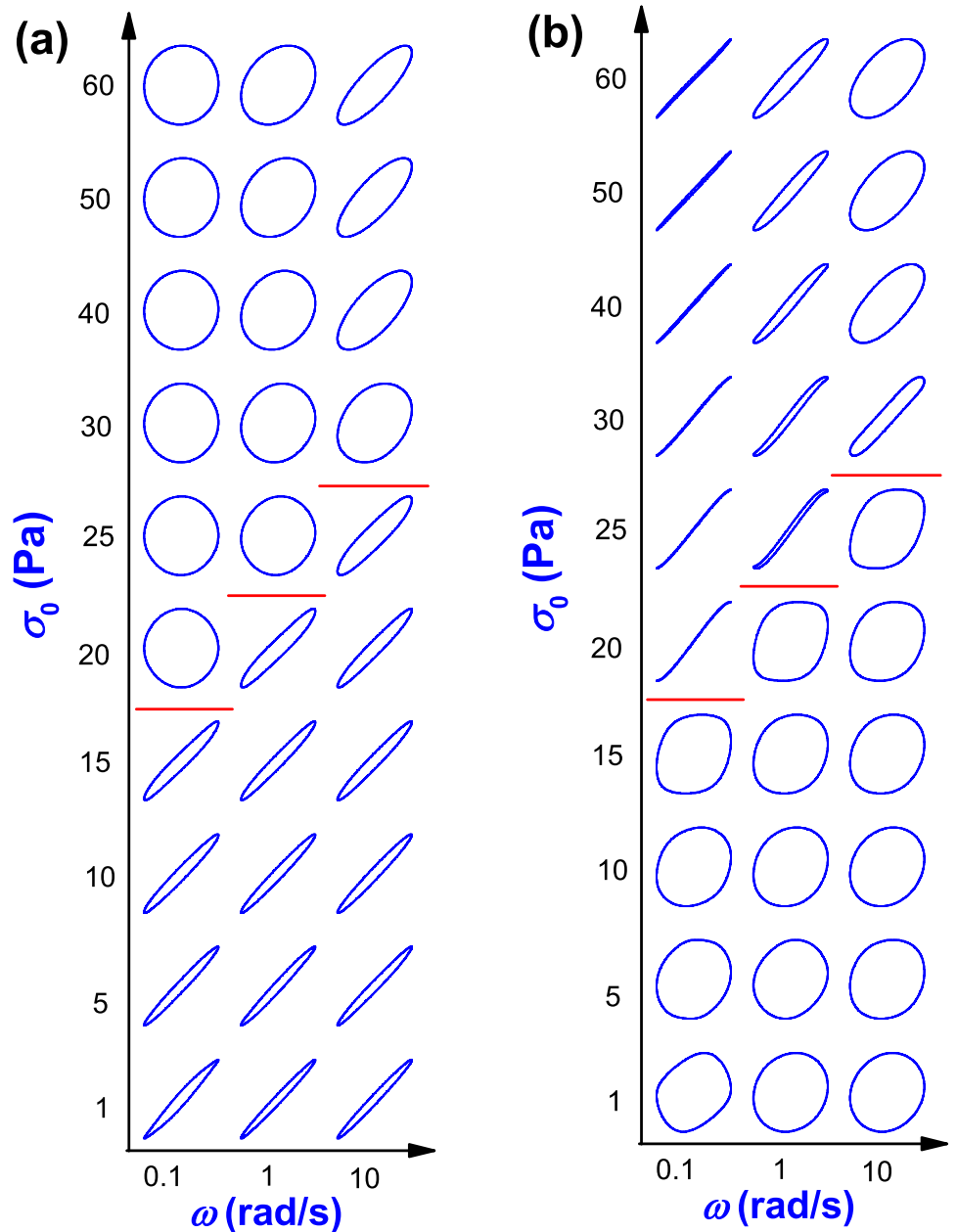

Fig. 15 Pipkin diagrams of the normalized elastic Lissajous curves $\gamma(t)/\gamma_0$ vs $\sigma(t)/\sigma_0$ (**a**) and normalized viscous Lissajous curves $\dot{\gamma}(t)/\dot{\gamma}_0$ vs $\sigma(t)/\sigma_0$ for gelled waxy crude oils formed at 11 °C

et al. 2013). The elastic and viscous Lissajous curves for the studied waxy crude oils in "Lissajous curves analysis" section were normalized in the form of $[\gamma(t)/\gamma_0 vs \sigma(t)/\sigma_0]$ and $[\dot{\gamma}(t)/\dot{\gamma}_0 vs \sigma(t)/\sigma_0]$, respectively. Then, the trajectories of each normalized elastic and viscous Lissajous curves were arranged in a two-dimensional Pipkin space according to the imposed values $\{\sigma_0, \omega\}$. The formed elastic Pipkin diagrams for the waxy crude oils are demonstrated in Fig. 15a, and the corresponding viscous Pipkin diagrams are displayed in Fig. 15b.

Through the normalized processing approach, the evolution characteristics of the resulting orbit shapes for the elastic and viscous Pipkin diagrams are consistent with the analysis for the elastic and viscous Lissajous curves in "Lissajous curves analysis" section, respectively. The yielding of waxy crude oils can be indicated by the marked line in Fig. 15 where an obvious transition for the Pipkin diagrams can be observed, and it is apparent that a higher imposed frequency typically results in a higher measured yield stress.

Conclusions

The gelled waxy crude oil can exhibit complex non-Newtonian rheological features including the transition from linear to nonlinear viscoelasticity. In the present work, the nonlinear viscoelastic characteristics of waxy crude oils were experimentally investigated by LAOStress techniques, and the following conclusions can be drawn:

Fourier transform results of I_{31} show that the nonlinear degree of waxy structure can be first strengthened and subsequently weakened as the imposed σ_0 increases. To be specific, with increasing σ_0, both c_3/c_1 and f_3/f_1 exhibit the first upward and then decreasing trends, indicating the first reinforced and subsequently weakened trends of elastic and viscous nonlinearities induced by the imposed σ_0, respectively. Furthermore, it is found that a lower applied ω tends to generate a more striking nonlinear response of waxy crude oils.

The variation characteristics of Lissajous curves further demonstrate a gradual destruction process with the increase in imposed σ_0 and a more significant flowability enhancement under a lower applied ω for the interlocking waxy network. In addition, larger viscoelastic measures and dissipated energy can be gained under a higher imposed σ_0 and a lower ω. Both the viscoelastic measures and third-order Chebyshev coefficients analysis signify the stress stiffening and stress thinning behaviors for waxy crude oils. The Pipkin diagrams were finally plotted to summarize and demonstrate the rich nonlinear viscoelastic characteristics of waxy crude oils, showing a higher measured yield stress under a higher imposed ω.

The present experimental results of LAOStress can, to some extent, provide support for the establishment of the elasto-viscoplastic constitutive model for waxy crude oils. Based on this, the model applications and predictions can be extended to the oscillatory test methods, serving for the development of more robust constitutive models.

References

Abivin P, Taylor SD, Freed D (2012) Thermal behavior and viscoelasticity of heavy oils. Energy Fuel 26:3448–3461

Andrade DEV, Cruz ACB, Franco AT, Negrão COR (2015) Influence of the initial cooling temperature on the gelation and yield stress of waxy crude oils. Rheol Acta 54:149–157

Atalık K, Keunings R (2004) On the occurrence of even harmonics in the shear stress response of viscoelastic fluids in large amplitude oscillatory shear. J Non-Newtonian Fluid Mech 122:107–116

Barnes HA (1997) Thixotropy-a review. J Non-Newtonian Fluid Mech 70:1–33

Carotenuto C, Grosso M, Maffettone PL (2008) Fourier transform rheology of dilute immiscible polymer blends: a novel procedure to probe blend morphology. Macromolecules 41:4492–4500

Chang C, Boger DV, Nguyen QD (1998) The yielding of waxy crude oils. Ind Eng Chem Res 37:1551–1559

Chang C, Nguyen QD, Rønningsen HP (1999) Isothermal start-up of pipeline transporting waxy crude oil. J Non-Newtonian Fluid Mech 87:127–154

Coutinho JAP, da Silva JAL, Ferreira A, Soares MR, Daridon J (2003) Evidence for the aging of wax deposits in crude oils by ostwald ripening. Pet Sci Technol 21:381–391

da Silva JAL, Coutinho JAP (2004) Dynamic rheological analysis of the gelation behaviour of waxy crude oils. Rheol Acta 43:433–441

Derec C, Ducouret G, Ajdari A, Lequeux F (2003) Aging and nonlinear rheology in suspensions of polyethylene oxide-protected silica particles. Phys Rev E 67:061403

Dimitriou CJ, Mckinley GH (2014) A comprehensive constitutive law for waxy crude oil: a thixotropic yield stress fluid. Soft Matter 10:6619–6644

Dimitriou CJ, Ewoldt RH, Mckinley GH (2013) Describing and prescribing the constitutive response of yield stress fluids using large amplitude oscillatory stress (LAOStress). J Rheol 57:27–70

Ewoldt RH, Clasen C, Hosoi AE, Mckinley GH (2007) Rheological fingerprinting of gastropod pedal mucus and synthetic complex fluids for biomimicking adhesive locomotion. Soft Matter 3:634–643

Ewoldt RH, Hosoi AE, Mckinley GH (2008) New measures for characterizing nonlinear viscoelasticity in large amplitude oscillatory shear. J Rheol 52:1427–1458

Ewoldt RH, Winter P, Maxey J, Mckinley GH (2010) Large amplitude oscillatory shear of pseudoplastic and elastoviscoplastic materials. Rheol Acta 49:191–212

Geri M, Venkatesan R, Sambath K, Mckinley GH (2017) Thermokinematic memory and the thixotropic elasto-viscoplasticity of waxy crude oils. J Rheol 61:427–454

Heymann L, Peukert S, Aksel N (2002) Investigation of the solid-liquid transition of highly concentrated suspensions in oscillatory amplitude sweeps. J Rheol 46:93–112

Hou L (2012) Experimental study on yield behavior of Daqing crude oil. Rheol Acta 51:603–607

Hyun K, Wilhelm M, Klein CO, Cho KS, Nam JG, Ahn KH, Lee SJ, Ewoldt RH, McKinley GH (2011) A review of nonlinear oscillatory shear tests: Analysis and application of large amplitude oscillatory shear (LAOS). Prog Polym Sci 36:1697–1753

Ilyin SO, Strelets LA (2018) Basic fundamentals of petroleum rheology and their application for the investigation of crude oils of different natures. Energy Fuel 32:268–278

Japper-Jaafar A, Bhaskoro PT, Sean LL, Sariman MZ, Nugroho H (2015) Yield stress measurement of gelled waxy crude oil: Gap size requirement. J Non-Newtonian Fluid Mech 218:71–82

Kallus S, Willenbacher N, Kirsch S, Distler D, Neidhöfer T, Wilhelm M, Spiess HW (2001) Characterization of polymer dispersions by Fourier transform rheology. Rheol Acta 40:552–559

Kané M, Djabourov M, Volle JL (2004) Rheology and structure of waxy crude oils in quiescent and under shearing conditions. Fuel 83:1591–1605

Koumakis N, Petekidis G (2011) Two step yielding in attractive colloids: transition from gels to attractive glasses. Soft Matter 7:2456–2470

Läuger J, Stettin H (2010) Differences between stress and strain control in the non-linear behavior of complex fluids. Rheol Acta 49:909–930

Leblanc JL (2008) Large amplitude oscillatory shear experiments to investigate the nonlinear viscoelastic properties of highly loaded carbon black rubber compounds without curatives. J Appl Polym Sci 109:1271–1293

Li C, Yang Q, Lin M (2009) Effects of stress and oscillatory frequency on the structural properties of Daqing gelled crude oil at different temperatures. J Pet Sci Eng 65:167–170

Lionetto F, Coluccia G, D'Antona P, Maffezzoli A (2007) Gelation of waxy crude oils by ultrasonic and dynamic mechanical analysis. Rheol Acta 46:601–609

Liu H, Lu Y, Zhang J (2018) A comprehensive investigation of the viscoelasticity and time-dependent yielding transition of waxy crude oils. J Rheol 62:527–541

Lopes-da-Silva JA, Coutinho JAP (2007) Analysis of the isothermal structure development in waxy crude oils under quiescent conditions. Energy Fuel 21:3612–3617

Macias-Rodriguez BA, Ewoldt RH, Marangoni AG (2018) Nonlinear viscoelasticity of fat crystal networks. Rheol Acta 57:251–266

Mendes R, Vinay G, Ovarlez G, Coussot P (2015) Modeling the rheological behavior of waxy crude oils as a function of flow and temperature history. J Rheol 59:703–732

Mendes R, Vinay G, Coussot P (2017) Yield stress and minimum pressure for simulating the flow restart of a waxy crude oil pipeline. Energy Fuel 31:395–407

Mujumdar A, Beris AN, Metzner AB (2002) Transient phenomena in thixotropic systems. J Non-Newtonian Fluid Mech 102:157–178

Paso K, Kompalla T, Oschmann HJ, Sjöblom J (2009) Rheological degradation of model wax-oil gels. J Dispers Sci Technol 30:472–480

Ptaszek P (2015) A geometrical interpretation of large amplitude oscillatory shear (LAOS) in application to fresh food foams. J Food Eng 146:53–61

Purnomo EH, Van Den Ende D, Mellema J, Mugele F (2006) Linear viscoelastic properties of aging suspensions. Europhys Lett 76:74–80

Rønningsen HP (1992) Rheological behaviour of gelled, waxy North Sea crude oils. J Pet Sci Eng 7:177–213

Stickel JJ, Knutsen JS, Liberatore MW (2013) Response of elastoviscoplastic materials to large amplitude oscillatory shear flow in the parallel-plate and cylindrical-couette geometries. J Rheol 57:1569–1596

Sun G, Zhang J (2015) Structural breakdown and recovery of waxy crude oil emulsion gels. Rheol Acta 54:817–829

Tarcha BA, Forte BPP, Soares EJ, Thompson RL (2015) Critical quantities on the yielding process of waxy crude oils. Rheol Acta 54:479–499

Ten Brinke AJW, Bailey L, Lekkerkerker HNW, Maitland GC (2007) Rheology modification in mixed shape colloidal dispersions. Part I: pure components. Soft Matter 3:1145–1162

Teng H, Zhang J (2013) Modeling the thixotropic behavior of waxy crude. Ind Eng Chem Res 52:8079–8089

Tiu C, Guo J, Uhlherr PHT (2006) Yielding behaviour of viscoplastic materials. Ind Eng Chem Res 12:653–662

Vinay G, Wachs A, Frigaard I (2007) Start-up transients and efficient computation of isothermal waxy crude oil flows. J Non-Newtonian Fluid Mech 143:141–156

Visintin RFG, Lapasin R, Vignati E, D'Antona P, Lockhart TP (2005) Rheological behavior and structural interpretation of waxy crude oil gels. Langmuir 21:6240–6249

Wang P, Liu J, Yu W, Zhou C (2011) Dynamic rheological properties of wood polymer composites: from linear to nonlinear behaviors. Polym Bull 66:683–701

Wardhaugh LT, Boger DV (1991) The measurement and description of the yielding behavior of waxy crude oil. J Rheol 35:1121–1156

Webber RM (2000) Yield properties of wax crystal structures formed in lubricant mineral oils. Ind Eng Chem Res 40:195–203

Wilhelm M, Maring D, Spiess HW (1998) Fourier-transform rheology. Rheol Acta 37:399–405

Yang H, Kang W, Zhao J, Zhang B (2015) Energy dissipation behaviors of a dispersed viscoelastic microsphere system. Colloids Surf A Physicochem Eng Asp 487:240–245

Yu W, Wang P, Zhou C (2009) General stress decomposition in nonlinear oscillatory shear flow. J Rheol 53:215–238